Persistent Spiral-Arm Structure of a Rotating Plasma in a Stationary Gas

T. Ikehata, H. Tanaka, N. Y. Sato, and H. Mase

Department of Electric and Electronic Engineering, Ibaraki University, Hitachi, Ibaraki 316-8511, Japan

(Received 26 February 1998)

A lagging-spiral-arm structure which is quite regular in shape and persists for a long time is observed when an argon plasma, rotating at a supersonic speed, is injected into an argon gas along a magnetic field line. As the gas pressure increases, two spirals develop due to the velocity shear at the plasma-gas interface, and the ions inside the plasma core are cross-field transported outward along the spirals, forming a low-density-halo region there. The velocity-shear-formation mechanism and the relation to other systems manifesting spiral structures are discussed. [S0031-9007(98)06966-X]

PACS numbers: 52.35.Py, 47.20.Ft, 52.30.–q

Collisionless plasma expansion across a magnetic field has been explored by many authors, in artificial release experiments in space [1,2], in laser explosion experiments [3–5], and in computer simulations [6–9]. Their attention is focused on the formation of a diamagnetic cavity and an instability evolving into regular and large-amplitude flute structures, e.g., free-streaming flutes or jets [3]; they are of current interest from the viewpoint of nonlinear self-organizing processes in continuous media.

In this Letter, we report a new plasma structuring: the lagging-spiral-arm structure, which is observed when a plasma rotating at a supersonic speed interacts with a stationary gas. The physical origin of the structuring is attributed to the centrifugal instability driven by the velocity shear at the plasma-gas interface and by the radial centrifugal force as previously demonstrated in systems of rotating liquids and gases [10–12]. The velocity-shear-generation mechanism proposed here is found to be successful in interpreting observations qualitatively. Figure 1 shows the schematic arrangement of experiment (GII device), whose details are documented in previous papers [13]. A rotating plasma is generated by a coaxial plasma gun installed at an end of a uniform magnetic field B_z of up to 3.6 kG. The argon gas puffed between the anode (25 mm o.d.) and cathode (10 mm o.d.) is rapidly ionized by firing a four-stage pulse forming network charged in 9 kV. The current pulse has an amplitude I of 10 kA and a duration of 30 μs. The operating pressure within the annular diode gap is estimated to be 10–20 mTorr, and the plasma is ejected in almost complete ionization. The Lorentz force $J_r B_z$ (J_r: the radial current density) sets the plasma into rigid rotation while the force $J_r B_\theta$ due to the self-induced magnetic field $B_\theta \propto I$ accelerates it along the axis. As a result, the plasma is ejected in the form of a rotating stream with both rotational and axial velocities v_θ and v_z. Prior to the experiment, the pressure in the chamber is below 3×10^{-6} Torr; thereafter, it is filled with an argon gas of pressure P_g from 1 to 500 mTorr. Time-resolved plasma images are taken with an image-converter camera (0.5 μs/frame and 0.1-μs exposure time) from the front and side directions of the plasma stream. The optical multichannel analyzer (OMA) is used to determine the rotational velocity from the Doppler shift of the spectral wavelength.

a. Plasma parameters and neutral collision parameters.—Typical plasma parameters for $I = 10$ kA, $B_z = 3.6$ kG in vacuum are the ion density $n_i = (4–10) \times 10^{14}$ cm^{-3}, the electron temperature $T_e \approx 10$ eV, the ion acoustic speed $c_s \equiv \sqrt{T_e/M_i} \approx 5 \times 10^3$ m/s (M_i: the ion mass), the rotational velocity $v_\theta \approx 9 \times 10^3$ m/s, the axial velocity $v_z \approx 2 \times 10^4$ m/s, the electron gyrofrequency $\Omega_e \approx 6 \times 10^{10}$ s^{-1}, the ion (Ar^+) gyrofrequency $\Omega_i \approx 9 \times 10^5$ s^{-1}, and the rotation frequency (on axis) $\omega \approx 1.2 \times 10^6$ s^{-1} ($\omega/\Omega_i \sim 1$). In addition, the electron gyroradius $\rho_e = v_{\mathrm{eth}}/\Omega_e \approx 3 \times 10^{-3}$ cm, the ion (Ar^+) gyroradius $\rho_i = v_\theta/\Omega_i \approx 1.0$ cm, the plasma core radius $r_c \approx 2$ cm, and the density-scale length $l_n \approx 0.8–1.2$ cm ($\rho_i/l_n \sim 1$).

(a) Electron-Ar^0 collisions are dominated by the elastic process since T_e is as low as 10 eV. The cross section σ_{en} becomes $\approx 2 \times 10^{-19}$ m^2 for $T_e \approx 10$ eV. Then the condition $\lambda_{en}/r_c = 1$ gives the filling gas pressure $P_g = 10$ mTorr. Here λ_{en} is the mean free path of electron-neutral collisions. (b) The cross section for Ar^+-Ar^0 collisions, σ_{in}, consists of elastic and charge-transfer processes and is given to be 6×10^{19} m^2 for 15 eV in the ion drift energy. The condition $\lambda_{in}/l_n = 1$ requires

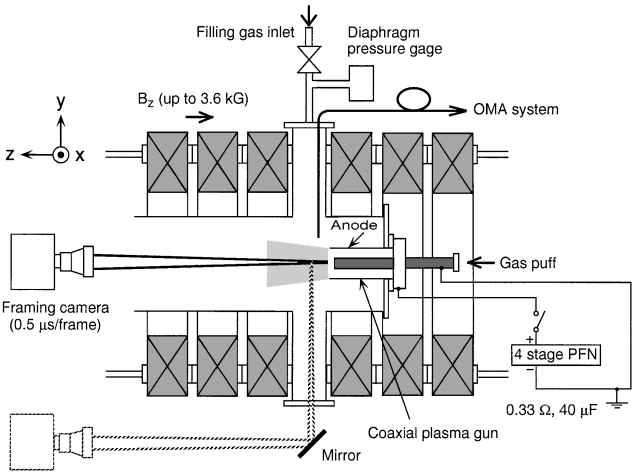

FIG. 1. Experimental arrangement.

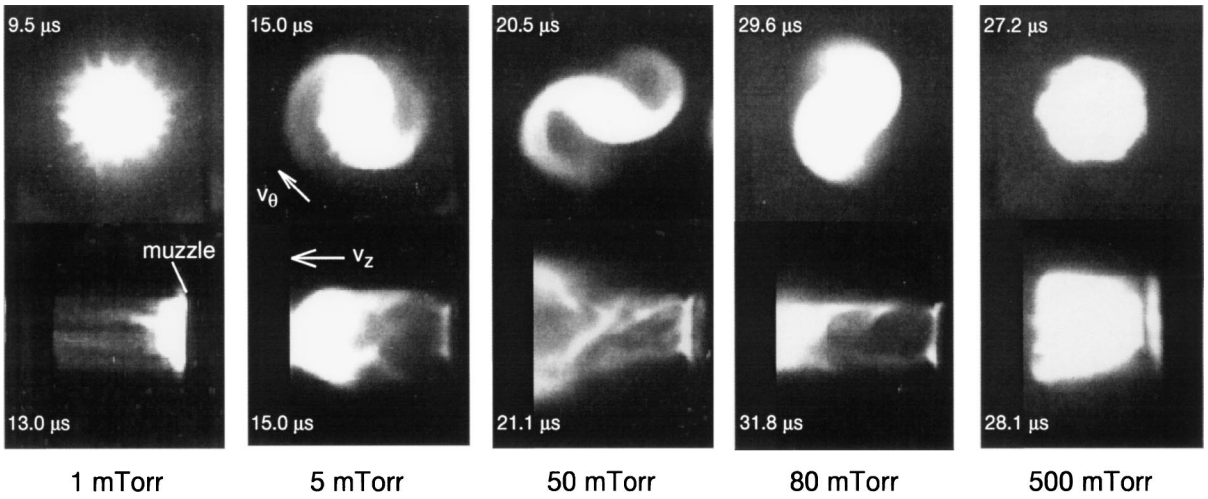

FIG. 2. Typical framing photographs for $P_g = 1$, 5, 50, 80, and 500 mTorr at $I = 10$ kA and $B_z = 3.6$ kG. The upper images are for the front view and the lower ones are for the side view.

$P_g = 6$ mTorr, where λ_{in} is the mean free path of ion-neutral collisions. (c) The mean free path for Ar^0-Ar^0 elastic collisions, λ_{nn}, is about 1 cm at 273 K and $P_g = 5$ mTorr; therefore, $\lambda_{nn}/l_n = 1$ applies at $P_g = 5$ mTorr.

b. Pressure dependence.—Typical framing images of rotating plasmas at $I = 10$ kA, $B_z = 3.6$ kG, and P_g from 1 to 500 mTorr are given in Fig. 2.

At $P_g = 1$ mTorr, the gas little affects plasma behavior. Short-wavelength–flute modes (the azimuthal mode number $m \approx 15$, $\lambda \approx 6$ mm) develop on the outer surface immediately after the plasma ejection just as observed in vacuum [13]. The relative amplitude of flutes, l_j/r_c (l_j: the amplitude of flutes) grows up to 0.5 in maximum in 10 μs. Thereafter, flutes appear to diffuse out and form a low-density-halo region around the plasma core. Since weak field-aligned striations observed in the side-on image imply that $k_\parallel \ll k_\perp$ and the structure is two dimensional, the instability is of flute mode. As P_g is increased to the range from 5 to 80 mTorr, flute modes are fully suppressed; instead, two pieces of lagging spirals ($m = 2$) develop on the outer boundary of the plasma. The relative amplitude of spirals is most appreciable at $P_g = 50$ mTorr. Suppression of flute modes is supposed to be due to collisional damping of electron drifts by electron-neutral collisions as predicted by Huba *et al.* [9] and observed by Ripin *et al.* [3]. The side-on image at 50 mTorr shows a pair of twisted arms or filaments around the axis. This suggests that spirals driven by the azimuthal velocity shear lag axially behind the plasma core proceeding at v_z. At $P_g = 500$ mTorr, both rotational and axial velocities decrease down to less than one-tenth of those in vacuum and become subsonic. The spiral-arm structure disappears; instead, a small-amplitude wavy pattern ($m \approx 8$) is recognized on the surface. It looks like Kelvin-Helmholtz vortices observed previously in fluid flows with the weak velocity shear [10,11].

Figure 3 summarizes P_g dependence of n_i, the neutral-to-ion density ratio n_n/n_i, v_θ, v_z, m, and l_j/r_c. Because the change in n_i is within a factor of 2, n_n/n_i changes from 0.1 to 50 approximately in proportion to P_g [Fig. 3(a)]. The hatched region corresponding to $P_g = 5$–10 mTorr denotes the threshold pressure over which neutral collisions become effective. Note that $n_n/n_i = 1$ at $P_g = 30$ mTorr. We define three regions, I, II, and III, with respect to the pressure. Figures 3(b) and 3(c) show v_θ and v_z as a function of P_g, respectively, where v_θ is evaluated from plasma framing images (circles) and from the Doppler shift of the ArII-480.601-nm line (squares). They are in fair agreement with each other, while v_z is derived from the time-of-flight (TOF) analysis of ion current signals. In region I, velocities v_θ and v_z are the same as those in vacuum and are supersonic. As P_g increases exceeding 5–10 mTorr, they start to decrease due to neutral collisions (region II) and become subsonic at $P_g = 100$ mTorr (region III). Figure 3(b) also suggests that v_θ in region I is limited to Alfvén's critical ionization velocity (CIV), $v_{cr} = 8.7 \times 10^3$ m/s (dashed line) [14]. Other solid curves in Figs. 3(b) and 3(c) are predictions from a plasma-gas-momentum-coupling model described later. From Fig. 3(d), there appear three instability structures, short-wavelength flutes, large-amplitude spirals, and small-amplitude vortices, characteristic of pressure regions I, II, and III, respectively. In other words, the structures are closely correlated with the degree of collisionality.

c. Origin of the flute structure.—The relative azimuthal drift v_d of magnetized electrons to unmagnetized ions on the plasma surface has been proposed as the mechanism of flute modes [1–6]. This drift gives rise to a diamagnetic current and leads to the formation of a diamagnetic cavity if the plasma beta is high enough. Here v_d is written as

$$v_d = -E/B + v_{ne} = v_g + v_{ni} + v_{ne}, \qquad (1)$$

where $v_g = Mg/eB$ is the gravitational drift velocity, $g = -dv_r/dt + \omega^2 r_c$, v_r is the radial expansion

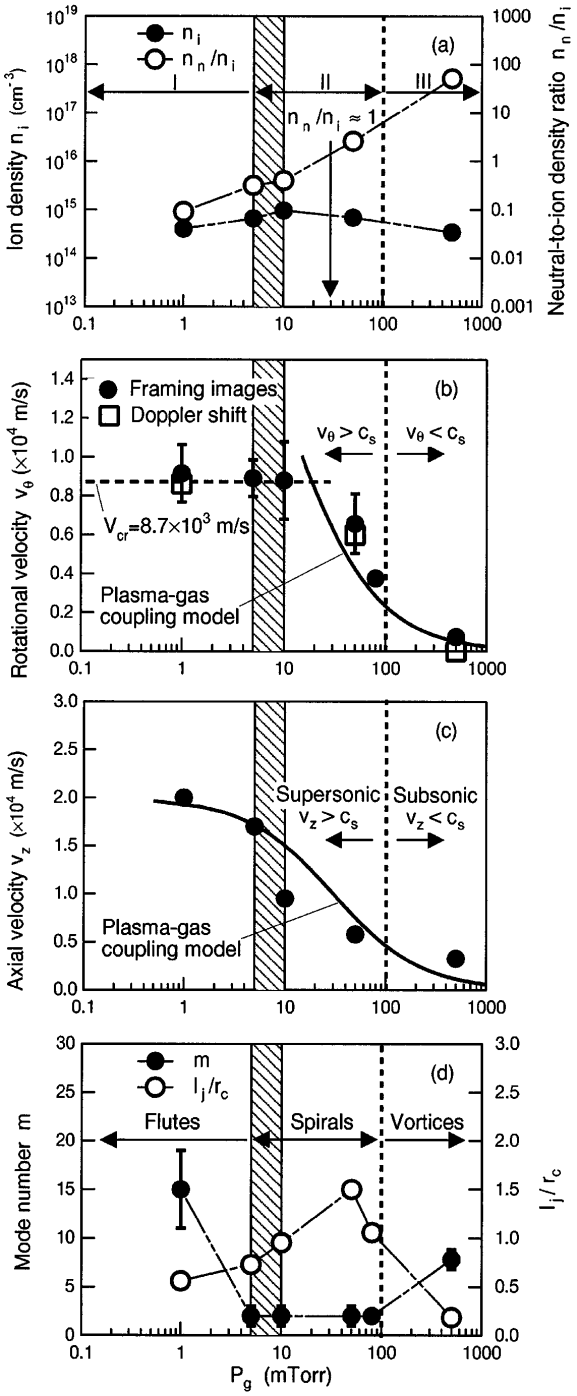

FIG. 3. P_g dependence of n_i, n_n/n_i, v_θ, v_z, m, and l_j/r_c.

velocity, and v_{ni} [v_{ne}] $= -(T_i/n_i eB)(\partial n_i/\partial r)$[$(T_e/n_e eB)(\partial n_e/\partial r)$] is the ion [electron] diamagnetic drift velocity. Previous investigations on the cross-field plasma expansion [1–5] are based on $g = -dv_r/dt$, while in the present investigation, the centrifugal acceleration $g = \omega^2 r_c$ primarily drives the instability ($\omega^2 r_c \approx 4 \times 10^9$ m/s$^2 > -dv_r/dt \approx (1-2) \times 10^9$ m/s^2). Characteristic features of the instability are (a) $k\rho_i \gg 1$, namely, the instability should be kinetic rather than fluidlike; (b) in the nonlinear region, the wavelength $2\pi/k \approx 0.6$ cm is nearly equal to $l_n = 0.8$–1.2 cm. They are quite similar to previous observations [3,6].

d. Origin of the spiral-arm structure.—The centrifugal instability [10–12] driven by both the velocity shear at the plasma-gas interface and the centrifugal force is proposed to be the origin. Convective rolls driven by the shear-driven instability are unfolded under the radial centrifugal force into a spiral form. The Kelvin-Helmholtz instability is destabilized at a subsonic speed of Mach number $M = v_\theta/c_s < 1$ and is fully stabilized at a supersonic speed of $M > 2\sqrt{2}$ [10]. In addition, Kelvin-Helmholtz instability does not depend on the sign of the velocity shear $\partial v_\theta/\partial r$. On the other hand, the centrifugal instability develops only when $M > 1$ and $\partial v_\theta/\partial r < 0$; namely, the inner part of a rotating fluid needs to move faster than the outer part. This condition is marginally satisfied in the present study because $M = v_\theta/c_s \geq 1.8$ is measured and the plasma core inside rotates faster than the surrounding gas. Characteristic features of observations are (a) the instability is fluidlike because the plasma is collisional; (b) two lagging spirals ($m = 2$) are formed over a wide range of parameters and have the largest amplitude near the condition $n_n/n_i = 1$; (c) the spiral-arm structure persists for a long time $\tau > 20$ μs, such that $\omega\tau/2\pi > 2.9$ and $\Omega_i\tau/2\pi > 2.9$; (d) a predicted large amplitude $l_j/\rho_i \gg 1$ [11] is marginally satisfied such that $l_j/\rho_i \approx 3$, $l_j/r_c \approx 1.5$.

Similarity among different physical systems which manifest spiral structures has been discussed by scientists of the former Soviet Union [10–12]. They showed a possibility that spiral arms of galaxies and spiral vortices in the rotating shallow water have the same origin: the centrifugal instability of two-dimensional, differentially rotating flows. Furthermore, Nezlin [11] suggested that the same structure should appear in plasmas also. Amagishi *et al.* [15] reported the spiral structure of a rotating mercury in a magnetic field. Morozov [12] analyzed hydrodynamic-instability-driven spiral modes in a galactic gas disk. He assumed a model that the inner part of the disk (R in radius and Ω_1 in angular frequency) rotates at a supersonic speed ($M \equiv \Omega_1 R/c_s > 1$) faster than the outer part (Ω_2) and a transition layer (or velocity-shear layer) of width L exists between them. Dispersion relations derived for $\Omega_2/\Omega_1 < 1$, $M > 1$, $L/R < 1$ predict the growth of spiral modes with m decreasing toward 2 with increasing M and L/R and with decreasing Ω_2/Ω_1. Especially in the case of our plasma conditions $\Omega_2/\Omega_1 = 0$, $M \approx 1.8$, and $L/R \sim 0.6$, it predicts $m = 2$; two spiral arms just observed. In the present experiment, spiral arms rotated at 0.33×10^6 rad/s, about a half of 0.8×10^6 rad/s of the plasma core ($P_g =$ 50 mTorr); this is reasonable because the center of the velocity-shear layer should rotate at $\Omega_1/2 = \omega/2$ if $\Omega_2 = 0$. It is worth noting that B_z makes the plasma structuring virtually two dimensional.

e. Possible mechanism of velocity shear.—Here we discuss the mechanism for generating the velocity shear by ion-neutral collisions. Because the ion and neutral

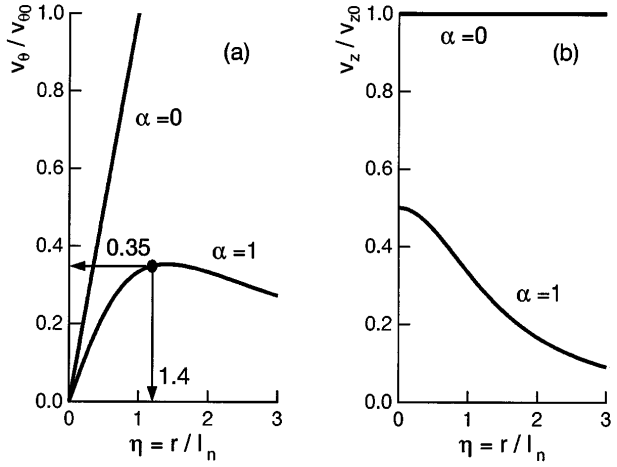

FIG. 4. (a),(b) Velocity-shear generation through the plasma-gas coupling.

have the same mass, the momentum of a moving ion is completely transferred to a neutral by one head-on collision. Then it may be reasonable to assume that plasma ions and neutrals are strongly coupled and have the same velocities v_θ and v_z. Let us consider how the velocity shear happens under the following model velocity and density distributions:

$$n_i(r) = \frac{n_0}{r^2/l_n^2 + 1}, \qquad n_n(r) = \alpha n_0,$$
$$v_{i\theta}(r) = \omega r, \qquad v_{n\theta}(r) = 0, \tag{2}$$
$$v_{iz}(r) = v_{z0}, \qquad v_{nz}(r) = 0,$$

where α is the initial neutral-to-ion density ratio at $r = 0$. After collisions, we have

$$v_\theta(r) = v_{i\theta}(r) = v_{n\theta}(r) = \frac{v_{\theta 0}}{\alpha} \frac{\eta}{\eta^2 + \delta}, \tag{3}$$

$$v_z(r) = v_{iz}(r) = v_{nz}(r) = \frac{v_{z0}}{\alpha} \frac{1}{\eta^2 + \delta}, \tag{4}$$

where $v_{\theta 0} \equiv l_n \omega$, $\eta \equiv r/l_n$, and $\delta \equiv 1 + 1/\alpha$. Model equations (3) and (4) were evaluated for parameters $\omega = 1.2 \times 10^6$ rad/s and $l_n = 1.2$ cm. Furthermore, we assumed $\eta = 1.67$ for Eq. (3) and $\eta = 0$ for Eq. (4) separately since v_θ was measured at the plasma core radius $r_c = 2$ cm so $\eta = r_c/l_n = 1.67$, while in the TOF measurement v_z should virtually be determined by bulk plasma ions located near the axis. Results have been plotted in Figs. 3(b) and 3(c) by solid lines. The agreement between the measurement and calculations is fairly good except that v_θ in region I is influenced by the CIV effect.

Equations (3) and (4) are plotted for $\alpha = 0$ ($P_g = 0$) and 1 ($P_g = 30$ mTorr) in Figs. 4(a) and 4(b). This figure shows that in the case of $\alpha = 1$, the maximum value of $v_\theta/v_{\theta 0}$ is limited to $1/2\alpha\sqrt{\delta} = 0.35$ at $\eta = \sqrt{\delta} = 1.4$ and the velocity-shear layer appears around $r = \sqrt{2}\, l_n = 1.7$ cm. Figure 5 shows velocity profiles measured by the Doppler shift for $P_g = 1$ mTorr ($\alpha =$ 0.033) and 50 mTorr ($\alpha = 1.67$). The velocity profile at 1 mTorr was almost the same as in vacuum; the plasma core is in rigid rotation with $\omega = 1.2 \times 10^6$ rad/s while the maximum velocity is limited to $v_{\rm cr}$. While P_g increases to 50 mTorr, ω decreases to 0.8×10^6 rad/s by 33% and the maximum velocity appearing at $x/l_n \approx 1$ also decreases to 5.4×10^3 m/s by 40%. In the region $x/l_n > 1$ the velocity decreases with x. These observations are in qualitative agreement with the above model and demonstrate that the velocity shear is generated near the plasma boundary.

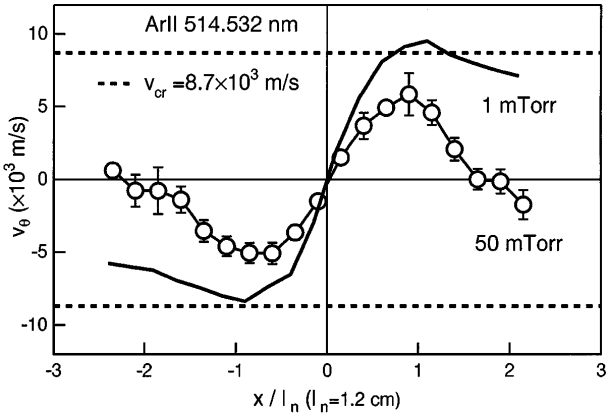

FIG. 5. Rotational velocity profiles for $P_g = 1$ and 50 mTorr; $v_{\rm cr}$ is the critical ionization velocity of Ar.

The authors acknowledge helpful discussions with Dr. K. Akimoto, Dr. H. Nakashima, Dr. M. Tanaka, and Dr. Y. Amagishi on the origin of flute modes and spiral structures.

[1] P. A. Bernhardt *et al.*, J. Geophys. Res. **92**, 5777 (1987).
[2] J. D. Huba, P. A. Bernhardt, and J. D. Lyon, J. Geophys. Res. **97**, 11 (1992).
[3] B. H. Ripin *et al.*, Phys. Fluids B **5**, 3491 (1993).
[4] G. Dimonte and L. G. Wiley, Phys. Rev. Lett. **67**, 1755 (1991).
[5] S. Okada, K. Sato, and T. Sekiguchi, J. Phys. Soc. Jpn. **46**, 355 (1979).
[6] K. Akimoto *et al.*, J. Geomagn. Geoelectr. **40**, 1161 (1988).
[7] R. D. Sydora *et al.*, Phys. Fluids **26**, 2986 (1983).
[8] D. Winske, Phys. Fluids B **1**, 1900 (1989).
[9] J. D. Huba, Phys. Fluids B **5**, 3491 (1993).
[10] A. M. Fridman *et al.*, Phys. Lett. **109A**, 228 (1985).
[11] M. V. Nezlin, E. N. Snezhkin, and A. C. Trubnikov, in *Proceedings of the International Conference on Plasma Physics, Kiev, 1987* (World Scientific, Singapore, 1987), p. 1184.
[12] A. G. Morozov, Sov. Astron. **23**, 278 (1979).
[13] T. Ikehata *et al.*, in *Proceedings of the International Conference on Plasma Physics, Foz do Iguacu, Brazil, 1994* (INPE, Brazil, 1995), Vol. 3, p. 173; T. Kikuchi *et al.*, J. Fac. Eng. Ibaraki Univ. **43**, 8 (1995).
[14] N. Brenning, IEEE Trans. Plasma Sci. **20**, 778 (1992).
[15] Y. Amagishi, Y. Yoshikawa, and J. Ohara, J. Phys. Soc. Jpn. **60**, 2496 (1992).